

# Conditions for Parametric and Free-Carrier Oscillation in SOI Ring Cavities with Active Carrier Removal

Ryan Hamerly, Meysam Namdari, Levon Mirzoyan, Dodd Gray, Christopher Rogers, and Kambiz Jamshidi *Member, IEEE*

**Abstract**—We model optical parametric oscillation in ring cavities, focusing on silicon at  $1.55\mu\text{m}$ , as a potential frequency-comb source for microwave and terahertz generation. Oscillation is possible if free-carrier absorption can be mitigated; this can be achieved using carrier sweep-out in a reverse-biased p-i-n junction to reduce the carrier lifetime. By varying the pump power, detuning, and reverse-bias voltage, it is possible to realize amplification in cavities with both normal and anomalous dispersion at a wide range of wavelengths including  $1.55\mu\text{m}$ . Furthermore, a free-carrier self-pulsing instability leads to rich dynamics when the carrier lifetime is sufficiently long.

**Index Terms**—Silicon photonics; Frequency comb; Nonlinear optics.

## I. INTRODUCTION

OPTICAL parametric amplification (OPA) and oscillation (OPO) are useful phenomena in optical fibers, silicon-nitride microrings, and  $\chi^{(2)}$  crystals, for such applications as frequency-comb generation [1], [2] and time-multiplexed optical logic [3]. Frequency combs generated from parametric oscillators can also be used as a source for tunable microwave or terahertz radiation [4], [5]. However, effectively utilizing parametric phenomena in silicon has been problematic because of two-photon absorption (TPA) and the resultant free-carrier absorption (FCA), and because waveguides fabricated on most silicon photonics processes do not have the anomalous dispersion required for phase matching [6]; these effects restrict OPA and OPO in waveguides to dispersion-engineered structures at mid-IR frequencies below the TPA cutoff [7].

These problems can be overcome using a microring cavity placed inside a reverse-biased p-i-n junction (Fig. 1). Active carrier removal, facilitated by the strong reverse-bias field in the junction [8], mitigates FCA by reducing the carrier lifetime by orders of magnitude. For a  $220\times 450$  nm waveguide, the lifetime varies between 5–100 ps, tunable by the bias voltage, and is 1–2 orders of magnitude smaller than the  $\sim 1$  ns

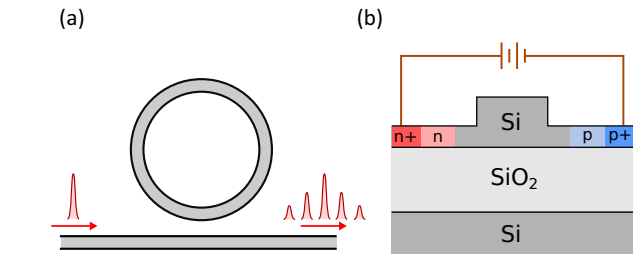


Fig. 1. (a) Illustration of the system: continuous-wave light enters the cavity and produces an output at multiple frequencies. (b) Cross-section of the device: an optical rib waveguide inside a reverse-biased p-i-n diode. The static electric field removes the photogenerated carriers, reducing their lifetime.

lifetimes observed in ordinary waveguides [9]. The phase-matching problem is solved using a cavity and appropriately detuning the pump field. This allows parametric gain even for rings with normal dispersion, something that is not possible with a single-pass approach.

This paper is organized as follows: in Sec. II, we introduce the mathematical model consisting of a Lugiato-Lefever equation with free-carrier terms. Sec. III treats the case of a continuous-wave pump and derives the conditions for parametric gain. These conditions are studied in both anomalous- and normal-dispersion rings, focusing on silicon at  $1.55\mu\text{m}$ . The gain profile and expected gain bandwidth are discussed in Sec. IV. Finally, Sec. V generalizes our discussion to the conditions for net gain at arbitrary wavelengths. Gain is possible at  $1.55\mu\text{m}$  with waveguide losses  $\lesssim 2$  dB/cm and carrier lifetimes  $\lesssim 100$  ps, and these bounds become much more lenient as one moves to longer wavelengths.

## II. MATHEMATICAL MODEL

To model this system, we use a normalized Lugiato-Lefever equation [10] with additional degrees of freedom for the free carriers [11]:

$$\frac{\partial \bar{a}}{\partial \bar{\tau}} = \left[ -\frac{1}{2} + i\bar{\Delta}_0 \right] \bar{a} - \frac{i\xi}{2} \frac{\partial^2 \bar{a}}{\partial \bar{t}^2} + \left[ (i-r)|\bar{a}|^2 + (-i-\mu^{-1})\bar{n}_c \right] \bar{a} + \sqrt{\eta} \bar{a}_{\text{in}} \quad (1)$$

$$\frac{d\bar{n}_c}{d\bar{\tau}} = \frac{1}{\bar{\tau}_c} \left[ \bar{\chi}_c \left( \frac{1}{t_R} \int_0^{t_R} |\bar{a}|^4 dt \right) - \bar{n}_c \right] \quad (2)$$

$$\bar{a}_{\text{out}} = -\sqrt{\eta} \bar{a} + \bar{a}_{\text{in}} \quad (3)$$

R. Hamerly was with the National Institute of Informatics, Tokyo, 101-8403 Japan. He is now with the Research Laboratory of Electronics at the Massachusetts Institute of Technology, Cambridge, MA, 02139 USA (email: rhamerly@mit.edu)

M. Namdari, L. Mirzoyan and K. Jamshidi are with the Integrated Photonic Devices Group, Technische Universität Dresden, Dresden, 01062 Germany (email: kambiz.jamshidi@tu-dresden.de)

D. Gray and C. Rogers are with the E. L. Ginzton Laboratory, Stanford University, Stanford, CA, 94305 USA (email: dodd@stanford.edu, cmrogers@stanford.edu)

Manuscript received January 31, 2018

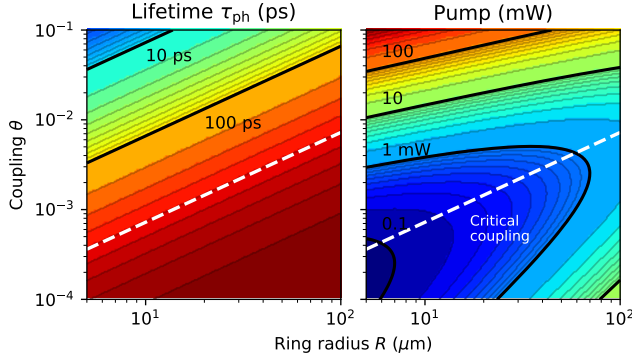


Fig. 2. Photon lifetime  $\tau_{\text{ph}}$  and pump scaling factor  $\mathcal{A}\eta^{-1}\xi_{\text{io}}^2$  (pump required to achieve  $\sqrt{\eta}\bar{a}_{\text{in}} = 1$ ) for a microring cavity with coupled to a waveguide, as a function of ring radius and coupling strength. Critical coupling is  $\eta = 1/2$ .  $\mathcal{A} = 0.1\mu\text{m}^2$ ,  $\alpha = 0.5$  dB/cm.

The dynamical variables are the (normalized) optical field  $\bar{a}(\bar{t}, \bar{\tau})$  and the carrier density  $\bar{n}_c(\bar{\tau})$ . The constants  $r = 0.2$  and  $\mu = 25$  are material parameters [12],  $\eta$  is the coupling efficiency (ratio of coupling to intrinsic loss),  $\xi \in \{-1, +1\}$  is the sign of the waveguide dispersion, the free-carrier dispersion term  $\bar{\chi}_c$  (given by  $\bar{\chi}_c = (\tau_c/\tau_{\text{ph}})(r\mu\sigma/2\hbar\omega\gamma v_g) \approx 10\tau_c/\tau_{\text{ph}}$ ) and carrier lifetime  $\tau_c$  can be tuned by the reverse bias voltage, and the cold-cavity detuning  $\bar{\Delta}_0$  can be tuned by the pump.

In (1-3), time is normalized to the photon lifetime  $\tau = \tau_{\text{ph}}\bar{\tau}$ , the field  $a = \xi_a\bar{a}$  is normalized to the strength of the Kerr nonlinearity, and the carrier density  $n_c = \xi_n\bar{n}_c$  is normalized to the strength of the free-carrier plasma dispersion (see Appendix A for details). Fig. 2 plots the lifetime and scale of the nonlinearity (pump power required to set  $\sqrt{\eta}\bar{a}_{\text{in}} = 1$ ) for a microring cavity with typical dimensions at  $1.55\mu\text{m}$  (cross-section area  $\mathcal{A} = 0.1\mu\text{m}^2$ , loss  $\alpha = 0.5$  dB/cm). Critically, pump powers are confined to a reasonable range  $\sim 0.1$ – $10$  mW for most structures, while photon lifetimes can vary in the range 10–400 ps. Note that the combination of low loss and efficient carrier sweep-out makes the carrier lifetime shorter than the photon lifetime  $\tau_c \lesssim \tau_{\text{ph}}$ , distinct from the condition  $\tau_c \gg \tau_{\text{ph}}$  typically encountered in integrated photonics.

### III. GAIN AND PHASE MATCHING

Now consider the case of parametric amplification  $2\omega_p \rightarrow \omega_s + \omega_i$ : the cavity is pumped at resonance  $\omega_p$ , and four-wave mixing creates photon pairs at signal and idler frequencies ( $\omega_s, \omega_i$ ). The circulating field takes the form:

$$\bar{a}(\bar{t}, \bar{\tau}) = a_p(\bar{\tau}) + a_s(\bar{\tau})e^{ik\bar{t}} + a_i(\bar{\tau})e^{-ik\bar{t}} \quad (4)$$

It is straightforward to derive equations for  $(a_p, a_s, a_i)$  by applying (4) to the Lugiato-Lefever equations (1-2). To assess whether parametric oscillation is possible, we first find the steady-state pump field by solving the bistability quintic

$$\eta|\bar{a}_{\text{in}}|^2 = \left[ \left( \frac{1}{2} + r|\bar{a}|^2 + \frac{\bar{\chi}_c}{\mu}|\bar{a}|^4 \right)^2 + \underbrace{\left( \bar{\Delta}_0 + |\bar{a}|^2 - \bar{\chi}_c|\bar{a}|^4 \right)^2}_{\bar{\Delta}} \right] |\bar{a}|^2 \quad (5)$$

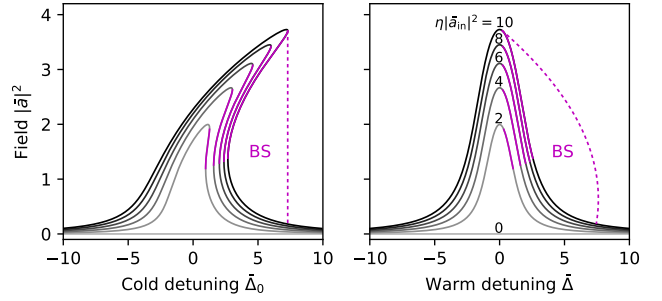


Fig. 3. Optical resonance and bistability, and difference between cold-cavity ( $\bar{\Delta}_0$ ) and warm-cavity ( $\bar{\Delta}$ ) detuning. Unstable solutions due to optical bistability (BS) are shown in pink.  $\lambda = 1.55\mu\text{m}$ ,  $\tau_c/\tau_{\text{ph}} = 0.1$ .

for the steady-state  $a_p$  (Fig. 3). We work in terms of the warm-cavity detuning  $\bar{\Delta} = \bar{\Delta}_0 + |\bar{a}|^2 - \bar{\chi}_c|\bar{a}|^4$  for convenience since cavity resonance occurs at  $\bar{\Delta} = 0$ .

Linearizing (1-2) in terms of  $(a_s, a_i)$  one determines stability. We find, in general, that the equations take the form:

$$\frac{d}{d\bar{\tau}} \begin{bmatrix} a_s \\ a_i^* \end{bmatrix} = M(a_p) \begin{bmatrix} a_s \\ a_i^* \end{bmatrix} \quad (6)$$

which is the expected form for a parametric oscillator. Once the form of  $M(a_p)$  is found, this has the following eigenvalues:

$$g = -\frac{1}{2} - 2r|a_p|^2 - \mu^{-1}\bar{\chi}_c|a_p|^4 \pm \sqrt{(1+r^2)|a_p|^4 - (\bar{\delta} + \frac{1}{2}\xi k^2)^2} \quad (7)$$

The parameter  $\bar{\delta} \equiv \bar{\Delta} + |a_p|^2$  denotes the phase mismatch. The gain in (7) is maximized under the *phase-matching condition*

$$-\frac{1}{2}\xi k^2 = \underbrace{\bar{\Delta} + |a_p|^2}_{\bar{\delta}} \quad (8)$$

The phase-matched case is treated in Sec. III-A, and the phase-mismatched case in Sec. III-B.

#### A. Phase-Matched Gain

To achieve phase matching,  $\bar{\delta}$  and  $\bar{\xi}$  must have opposite sign. For  $\bar{\delta} < 0$  this requires normal dispersion, while for  $\bar{\delta} > 0$  this requires anomalous dispersion. Note that this differs from single-pass parametric amplification, where phase matching is only possible with anomalous dispersion. Here it can occur for normal dispersion as well, thanks to the detuning of the cavity.

With phase matching, the gain  $g$  (called  $g_{\text{max}}$ ) is given by the formula:

$$g_{\text{max}} = -\frac{1}{2} + (\sqrt{1+r^2} - 2r)|a_p|^2 - \mu^{-1}\bar{\chi}_c|a_p|^4 \quad (9)$$

Figure 4 shows the phase-matched gain  $g_{\text{max}}$  as a function of pump intensity  $\eta|\bar{a}_{\text{in}}|^2$  and warm-cavity detuning  $\bar{\Delta}$ . Parametric oscillation occurs to the right of the red curve  $g_{\text{max}} = 0$ , as long as phase-matching is satisfied. The plots are color-coded according to whether phase-matching requires

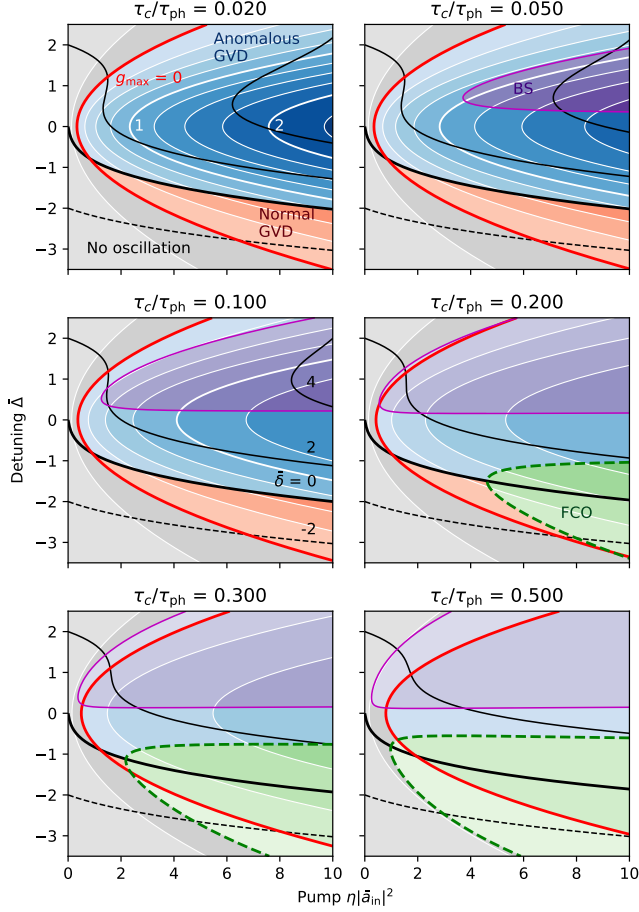


Fig. 4. Phase-matched gain  $g_{\max}$  (red and white contours) and  $\bar{\delta}$  (black contours) as a function of pump power and detuning. Blue and red regions indicate anomalous and normal GVD. Optical bistability (BS) and free-carrier oscillations (FCO) are given in the purple and green regions.

anomalous dispersion ( $\bar{\delta} > 0$ , blue) or normal dispersion ( $\bar{\delta} < 0$ , red).

Maximizing over  $|a_p|^2$  and substituting  $\bar{\chi}_c$ , we see that the optimal gain is:

$$g = \frac{1}{2} \left[ \frac{(\sqrt{1+r^2} - 2r)^2 \hbar \omega \gamma v_g \tau_{\text{ph}}}{r\sigma \tau_c} - 1 \right] \quad (10)$$

Taking values from Appendix A, we get:

$$g = \frac{1}{2} \left[ 0.65 \frac{\tau_{\text{ph}}}{\tau_c} - 1 \right] \quad (11)$$

This gives a strict condition for OPO, namely, gain will only occur if the ratio of carrier to photon lifetime is  $\tau_c/\tau_{\text{ph}} \lesssim 0.65$ . As discussed in Sec. II, this ratio is usually  $\gg 1$  in silicon photonic structures, but the p-i-n carrier sweep-out allows it to approach  $\lesssim 0.1$ , tunable by the voltage applied to the diode. This allows p-i-n structures to realize OPO in silicon at  $1.55\mu\text{m}$ , which is not possible otherwise in silicon.

Because bistability (BS) and free-carrier oscillations (FCO) can complicate things [13], [14], these effects are also plotted in Fig. 4. The solutions in the purple region are unstable because the bistability quintic bends over (Fig. 3). Free-carrier

oscillations are shown in green. These regions are determined by taking the  $3 \times 3$  Jacobian matrix  $J$  of (1-2) and searching for the conditions [14]:

$$\underbrace{\det(J) > 0}_{\text{BS}}, \quad \underbrace{(\text{tr}(J)^2 - \text{tr}(J^2))\text{tr}(J) - 2\det(J) > 0}_{\text{FCO}} \quad (12)$$

Parametric gain is dominant when the carrier lifetime is very small, while free-carrier oscillations take over for longer carrier lifetimes (comparable to the photon lifetime). By tuning the carrier lifetime, one can selectively activate either OPO gain or free-carrier oscillations. Thus a single cavity could be used to see both effects.

### B. Phase-Mismatched Gain

Of course, the full phase-matched gain is only possible when condition (8) is satisfied. For various reasons (e.g. wrong dispersion, discretization of  $k$  due to boundary conditions) phase-matching may not hold exactly. In this case, we need to use the more general formula (7). The gain spectrum  $g(k)$  is plotted for a range of parameters ( $\bar{\Delta}$ ,  $\bar{a}_{\text{in}}$ ) in Fig. 5. The optimal gain is found by maximizing (7) over  $k$ . The result depends on the sign of  $\xi$ :

$$k_{\max} = \begin{cases} \pm \sqrt{2|\bar{\delta}|} & \text{sgn}(\xi) = -\text{sgn}(\bar{\delta}) \\ 0 & \text{sgn}(\xi) = +\text{sgn}(\bar{\delta}) \end{cases} \quad (13)$$

For the case  $\text{sgn}(\xi) = +\text{sgn}(\bar{\delta})$  where phase matching is not possible,  $g$  is maximized for  $k = 0$ . But this mode can't be amplified (it is the pump mode); instead the closest resonant sidebands experience maximum gain.

Although phase-matching certainly *helps* one achieve gain, the key message from Figs. 5-6 is that it is not *necessary*. In particular, for  $\tau_c/\tau_{\text{ph}} \lesssim 0.200$  in Fig. 6, a large part of the region  $\bar{\delta} > 0$  experiences gain for normal group-velocity dispersion (GVD), even though phase matching is not

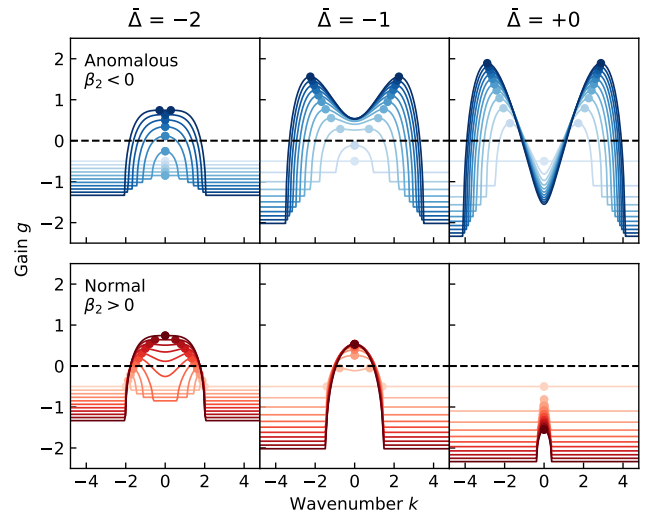


Fig. 5. Parametric gain  $g(k)$  for various detuning, pump power, and dispersion values. Power ranges from  $\eta|\bar{a}_{\text{in}}|^2 = 0$  (light) to  $\eta|\bar{a}_{\text{in}}|^2 = 10$  (dark). Carrier lifetime  $\tau_c/\tau_{\text{ph}} = 0.05$ . Dots give  $k$  at optimal gain (13)

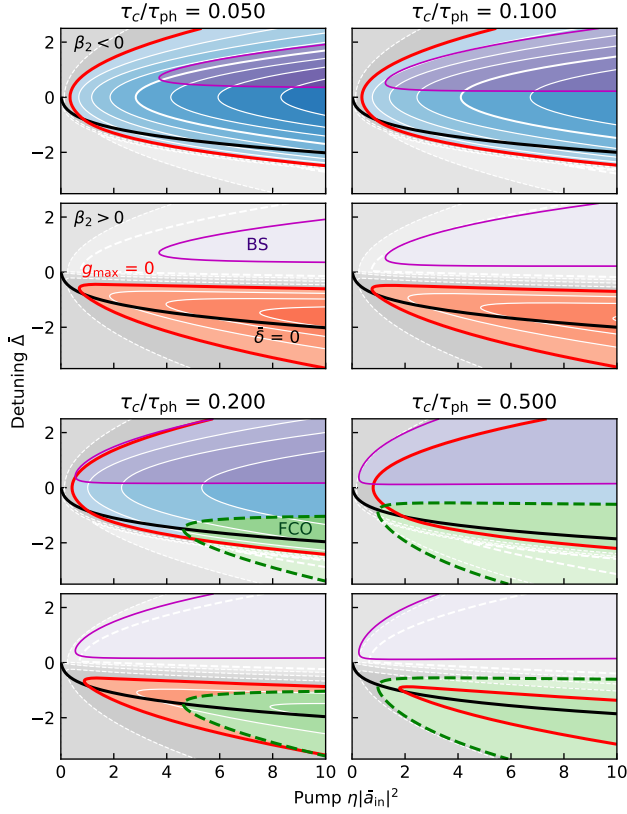


Fig. 6. Optimal gain for cavities with anomalous dispersion (blue) and normal dispersion (red).

satisfied ( $\text{sgn}(\xi) = \text{sgn}(\bar{\delta}) = +1$ ). This is important from an engineering standpoint, since the zero-dispersion wavelength for ridge waveguides as in Fig. 1(b) is typically  $\lambda_{\text{ZDM}} \gtrsim 2\mu\text{m}$  [15], and in many multi-project wafer photonics processes, the permitted waveguide dimensions do not allow for anomalous GVD.

From Fig. 5, we see that the gain profile is very dispersion-dependent. As expected, for positive or zero detuning, the gain spectrum is double-peaked for anomalous dispersion – since the phase mismatch  $\bar{\delta} > 0$  can be cancelled by dispersion. For normal dispersion, it is single-peaked because phase-matching cannot be achieved and the phase mismatch is minimized by setting  $k = 0$ . For sufficiently negative detuning ( $\bar{\delta} < 0$ ), the story is reversed (a similar effect occurs in conventional  $\chi^{(2)}$  OPOs [16]).

#### IV. MODES AND GAIN BANDWIDTH

Sec. III (in particular Fig. 5) calculated the gain as a function of wavenumber  $k$ . Oscillation is assumed to happen as long as some value of  $k$  has net round-trip gain. However, this assumes that the cavity has a resonance at the optimal  $k$ , which in turn depends on the spacing of the modes. If the mode spacing is too large, then we may not see oscillation at all, since all the modes may live outside the oscillation region.

The normal mode spacing is computed from the periodic boundary condition on  $t$ ; cast into unitless variables  $t =$

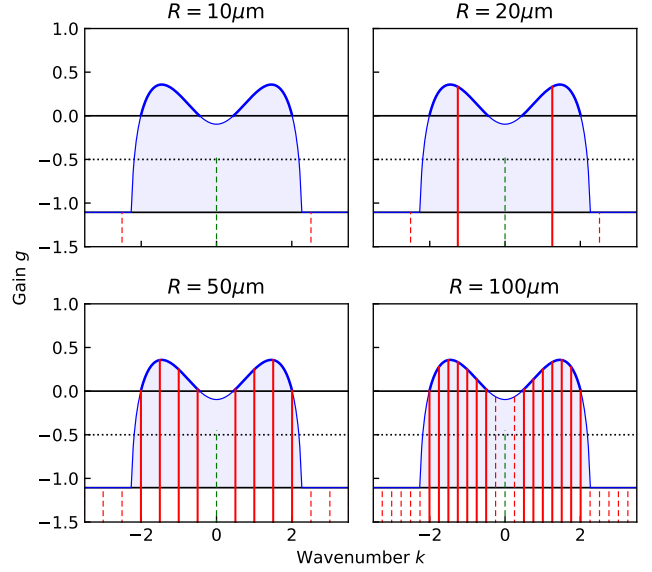


Fig. 7. Gain for normal modes in ring cavities with radii  $R = 10\mu\text{m}$ ,  $20\mu\text{m}$ ,  $50\mu\text{m}$ ,  $100\mu\text{m}$ . Parameters:  $\xi = +1$ ,  $\bar{\Delta} = -2.5$ ,  $\eta|a_{\text{in}}|^2 = 10$ ,  $\tau_c/\tau_{\text{ph}} = 0.05$ ,  $\tau_{\text{ph}} = 1$  ns.

$\sqrt{|\beta_2|v_g\tau_{\text{ph}}\bar{t}}$ , the unitless  $\bar{t}$  has a period of  $t_R/\sqrt{|\beta_2|v_g\tau_{\text{ph}}}$ . One can write the field as a Fourier series  $\bar{a}(\bar{\tau}, \bar{t}) = \sum_m \bar{a}_m(\bar{\tau})e^{im\bar{K}\bar{t}}$  where the normalized free-spectral range  $\bar{K}$  is given by

$$\bar{K} = 2\pi \frac{\sqrt{|\beta_2|v_g^3\tau_{\text{ph}}}}{L} \quad (14)$$

This is the spacing between the modes in Fig. 7. Since the gain region tends to live around  $|k| \lesssim 1$ , this means that gain will be excluded if  $\bar{K} \gg 1$  simply because no normal mode lies in the gain region. Typical  $450 \times 220$ -nm waveguides have a GVD of  $\beta_2 \approx +1 \text{ ps}^2/\text{m}$  [17, Ch. 11]. For a ring cavity, this gives  $\bar{K} \approx 25(\tau_{\text{ph}}/\text{ns})^{1/2}(R/\mu\text{m})^{-1}$ , which suggests a cavity with radius  $R \gtrsim 25\mu\text{m}$ , consistent with Fig. 7.

In normalized units, the bandwidth of the gain window is  $|k| \lesssim 1$ ; in real units, this is:

$$|\Delta\omega| \lesssim \frac{1}{\sqrt{|\beta_2|v_g\tau_{\text{ph}}}} \approx 2\pi \times (500 \text{ GHz}) \frac{1}{\sqrt{\tau_{\text{ph}}/\text{ns}}} \quad (15)$$

which suggests that if a frequency comb can be stabilized, the bandwidth could be  $\gtrsim$  THz and pulses could be around  $\lesssim$  1ps long. Waveguide dispersion engineering would further improve this figure.

#### V. WAVELENGTH DEPENDENCE

As the operating wavelength is increased  $n_2$  grows while two-photon absorption  $\beta$  is either reduced or eliminated; consequently the conditions for parametric amplification are relaxed. This is why amplification can be observed at  $\gtrsim 2.0\mu\text{m}$  in ordinary structures without p-i-n sweepout [18]. This section derives the general conditions in which amplification is possible, in terms of wavelength  $\lambda$ , waveguide loss  $\alpha$  and carrier lifetime  $\tau_c$ .



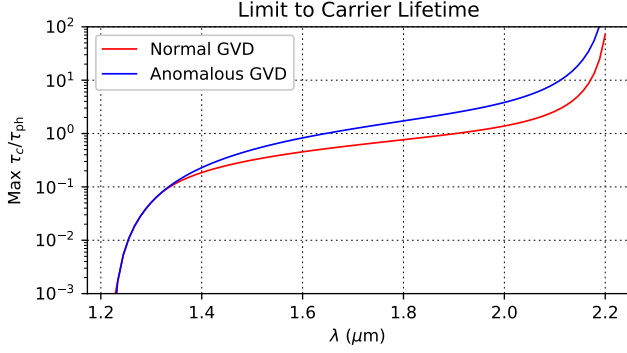


Fig. 8. Carrier-lifetime limit from Eq. (16): if  $\tau_c/\tau_{ph}$  exceeds this amount, parametric oscillation is impossible.

### A. Limit on Carrier Lifetime

Condition (10) sets the maximum carrier lifetime (relative to photon lifetime) required to achieve positive gain:

$$(\tau_c/\tau_{ph})_{\max} = \frac{(\sqrt{1+r^2}-2r)^2 \hbar \omega \gamma v_g}{r \sigma} \quad (16)$$

This quantity is wavelength-dependent (blue curve in Fig. 8). This limit is applicable in the anomalous-dispersion regime, where an oscillation region always exists around  $\bar{\Delta} = 0$  if  $\tau_c/\tau_{ph} < (\tau_c/\tau_{ph})_{\max}$  (see Fig. 6).

In the normal-dispersion case there is a more stringent bound set by free-carrier oscillations. Fig. 6 shows that for  $\tau_c/\tau_{ph} = 0.50$ , it is impossible to reach the (red) parametric-gain region without first crossing into the (green) FCO region. Once the free-carrier oscillations start, they disrupt the parametric process and suppress gain. The FCO region overtakes the gain region roughly when the red ( $g_{\max} = 0$ ), black ( $\bar{\delta} = 0$ ) and green lines in Fig. 6 intersect at the same point. This is easy to find numerically, and is plotted in the Fig. 8 (red curve).

Note that the maximum  $\tau_c$  always scales with  $\tau_{ph} = (1 - \eta)/\alpha v_g$ , which in turn scales as  $\alpha^{-1}$ . Long carrier lifetimes can be alleviated with very low-loss structures; likewise high loss can be compensated with short carrier lifetimes.

### B. Limit on Waveguide Loss

We can derive an upper bound on  $\alpha$  that arises from screening of the free-carrier sweepout field. Fig. 9 illustrates the screening effect for a 2D waveguide: at large field intensities, since the extraction process is not instantaneous, the steady-state carrier distribution effectively screens the reverse-bias field [19]. If this screening reduces the internal field to near zero, carrier sweep-out will be ineffective.

A full treatment of screening requires sophisticated 2D transport simulations [9]; however, a reasonable analytic esti-

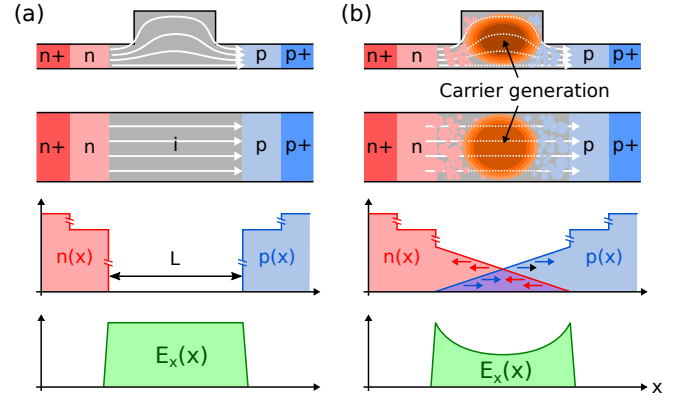


Fig. 9. Illustration of free-carrier sweep-out field screening. State of waveguide with (a) weak field and (b) strong field generating carriers. Top to bottom: 2D model of waveguide. Approximate 1D model. Steady-state carrier densities  $n(x), p(x)$  in 1D model. Steady-state electric field  $E_x(x)$  in 1D model.

mate can be derived by approximating the waveguide as a 1D system. The transport equations become:

$$\frac{\partial p}{\partial t} = G(x) - \frac{\partial}{\partial x} (v_p(E_x)p) \quad (17)$$

$$\frac{\partial n}{\partial t} = G(x) + \frac{\partial}{\partial x} (v_n(E_x)n) \quad (18)$$

$$\frac{\partial E_x}{\partial x} = \frac{e}{\epsilon_0} (p - n) \quad (19)$$

To minimize the carrier lifetime, p-i-n structures are strongly reverse-biased, so the electron and hole drift velocities are close to the saturation velocity  $v_{\text{sat}} \approx 10^7 \text{ cm/s}$  [20]. Assuming a uniform carrier generation rate  $G$ , the steady-state carrier concentrations are  $p = Gx/v_{\text{sat}}$ ,  $n = G(L-x)/v_{\text{sat}}$ , where  $L$  is the spacing between the doped regions. Further assuming that the voltage drop across the doped regions is small compared to the drop across the intrinsic region (so  $\int_0^L E_x dx = V_0$ ), we find:

$$E_x = \left( \frac{V_0}{L} - \frac{eGL^2}{12\epsilon_0 v_{\text{sat}}} \right) + \frac{eG}{\epsilon_0 v_{\text{sat}}} (x - L/2)^2 \quad (20)$$

This field is minimized at the center of the waveguide. Screening will be effective when  $E_x(L/2) \approx 0$ , which limits the generation rate to:

$$G \lesssim \frac{12\epsilon_0 v_{\text{sat}} V_0}{eL^3} \quad (21)$$

For typical p-i-n parameters ( $L = 1 \mu\text{m}$ ,  $V_0 = 15 \text{ V}$ ), one finds  $G \lesssim 10^{27} \text{ cm}^{-3} \text{ s}^{-1}$ , which corresponds to  $I \lesssim 4 \times 10^8 \text{ W/cm}^2$  at  $1.55 \mu\text{m}$ . Numerical simulations for waveguides of this size confirm that this is the region in which carrier sweepout is effective [9].

Recall that the phase-matched OPA gain depends only on the circulating power through Eq. (9). In normalized units, the gain threshold depends only on the constant  $r$  and the ratio  $\zeta = \tau_c/\tau_{c,\max}$ :

$$|\bar{a}|^2 = \frac{1}{\sqrt{1+r^2}-2r} \underbrace{\frac{1-\sqrt{1-\zeta}}{\zeta}}_{f(\zeta)} \quad (22)$$

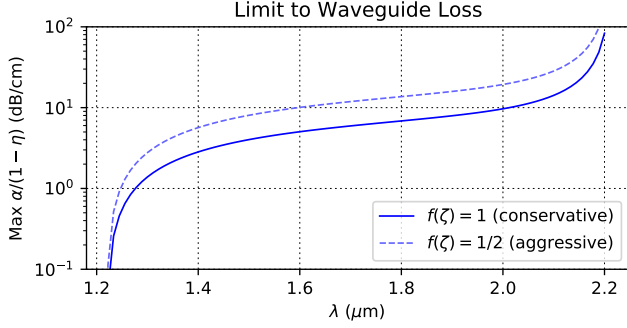


Fig. 10. Field-screening limit to waveguide loss  $\alpha$  as a function of wavelength, Eq. (24). ( $V_0 = 15\text{V}$ ,  $L = (\lambda/1.55)$ ).

where the  $\zeta$ -dependent term limits to  $f(\zeta) = \frac{1}{2}$  for  $\zeta \ll 1$  ( $\tau_c \ll \tau_{c,\text{max}}$ ) and  $f(\zeta) = 1$  at  $\zeta = 1$  ( $\tau_c = \tau_{c,\text{max}}$ ).

Scaling to dimensional units (Appendix A), we find that the circulating intensity at threshold scales with  $\alpha$ :

$$I = |a|^2 = \frac{\alpha}{\gamma(1-\eta)(\sqrt{1+r^2}-2r)} \frac{1-\sqrt{1-\zeta}}{\zeta} \quad (23)$$

Since the carrier generation rate for two-photon absorption is  $G = \beta I^2/2\hbar\omega = (r\gamma/\hbar\omega)I^2$ , one can bound  $\alpha$  using (21):

$$\alpha \lesssim \frac{(1-\eta)(\sqrt{1+r^2}-2r)}{f(\zeta)} \left[ \frac{12\epsilon_0\hbar\omega\gamma v_{\text{sat}}V_0}{reL^3} \right]^{1/2} \quad (24)$$

This is plotted in Fig. 10. Note that bound is on the effective loss per unit length due to *both* input/output coupling and intrinsic roughness / absorption. Thus, the bound on  $\alpha$  scales as  $(1-\eta)$ , which becomes stricter the more over-coupled a cavity is. At  $2\mu\text{m}$ , the bound is very loose (tens of dB/cm), but at telecom wavelengths is of order a few dB/cm, depending on the cavity coupling.

Conditions (16) and (24) are plotted together in Fig. 11. This provides a comprehensive picture of the design requirements for parametric oscillation in ring cavities with active carrier removal. While the requirements for long-wavelength oscillation are relatively loose, oscillation at or below  $1.55\mu\text{m}$  require both low-loss structures ( $\lesssim 2\text{--}3\text{dB/cm}$ ) with short carrier lifetimes ( $\lesssim 100\text{ps}$ ), which will require careful engineering of the fabrication process and resonator design.

## VI. CONCLUSION

We have studied the conditions for parametric oscillation in silicon microring cavities, focusing primarily on phenomena at  $1.55\mu\text{m}$ , but with an analysis that generalizes to all wavelengths. Parametric oscillations should allow the formation of frequency combs, which could be a useful resource for microwave or terahertz generation. The key advances that make this possible are carrier sweep-out using a p-i-n junction, which reduces carrier lifetimes and the resultant free-carrier absorption; and the use of a detuned microring cavity rather than a single-pass waveguide, which allows for gain and oscillation even under normal dispersion.

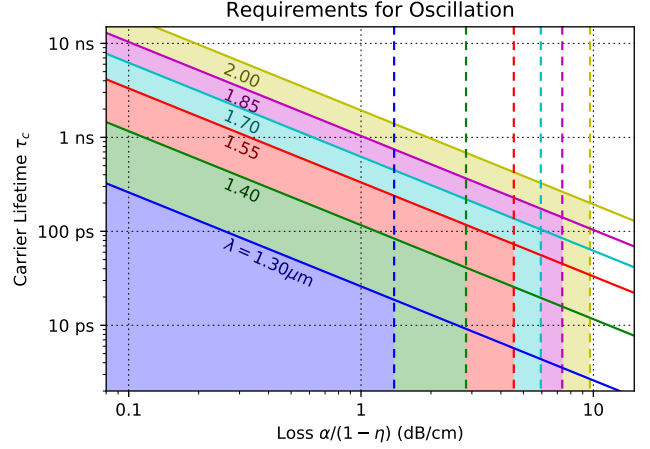


Fig. 11. Silicon ring-resonator conditions for parametric oscillation. Solid lines denote limit Eq. (16), while dashed lines denote limit Eq. (24) ( $f(\zeta) = 1$ ,  $V_0 = -15\text{V}$ ,  $L = \lambda/1.55$ ).

TABLE I  
CONSTANTS USED IN NORMALIZED LUGIATO-LEFEVER EQUATION

Normalization Constants		
$\xi_a = (\gamma v_g \tau_{\text{ph}})^{-1/2}$		Circulating field
$\xi_n = 2/\mu\sigma v_g \tau_{\text{ph}}$		Carrier density
$\xi_{i/o} = \sqrt{t_R/\gamma v_g \tau_{\text{ph}}^2}$		Input/output field
$\xi_t = \sqrt{ \beta_2 v_g \tau_{\text{ph}}}$		Fast time
Material Constants and Values at $1.55\mu\text{m}$		
$r = \beta\lambda/4\pi n_2$	0.189	TPA / Kerr ratio
$\gamma = 2\pi n_2/\lambda$	$3.9 \cdot 10^{-9}\text{cm/W}$	Nonlinear refraction
$\mu = \frac{4\pi}{\lambda} \frac{dn/dn_c}{d\alpha/dn_c}$	25	FCD / FCA ratio
$\sigma = d\alpha/dn_c$	$1.45 \cdot 10^{-17}\text{cm}^2$	FCA cross section

With typical silicon waveguide dimensions, it should be possible to form combs at  $1.55\mu\text{m}$  with bandwidths  $\gtrsim\text{THz}$ , with the number of comb lines set by the ring radius. Proper dispersion engineering could enable broader combs. The gain profile can be tuned with the pump power and frequency, as well as the p-i-n bias voltage, which sets the carrier lifetime.

For long carrier lifetimes  $\tau_c/\tau_{\text{ph}} \gtrsim 0.2$ , free-carrier oscillations compete with parametric gain. A more complete study will require full numerical simulations and merits separate discussion.

## APPENDIX A PARAMETERS IN NORMALIZED LLE

The terms in the Lugiato-Lefever Equation (LLE) are normalized according to:  $a = \xi_a \bar{a}$ ,  $n_c = \xi_n \bar{n}_c$ ,  $a_{i/o} = \xi_{i/o} \bar{a}_{i/o}$ ,  $t = \xi_t \bar{t}$ ,  $\tau = \tau_{\text{ph}} \bar{\tau}$ . Here  $|a|^2$  and  $|a_{i/o}|^2$  are intensities (units  $\text{W/cm}^2$ ) and  $n_c$  is a carrier density (units  $\text{cm}^{-3}$ ). The normalization constants are given in Table I.

The material constants in Table I depend on the nonlinear index  $n_2$ , two-photon absorption  $\beta$ , and free-carrier index change and absorption  $dn/dn_c$ ,  $d\alpha/dn_c$  (electrons plus holes), which are tabulated in the literature. Both  $\gamma$  and  $r$  depend

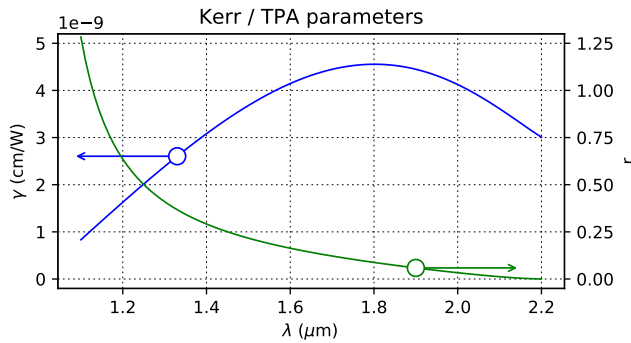


Fig. 12. Scaling of Kerr and TPA parameters  $\gamma$  and  $r$  with wavelength.

nontrivially on  $\lambda$  (Fig. 12, see [17, Sec. 11.4] and references); for  $\mu$  and  $\sigma$  we use the Drude-model scaling:

$$\mu \propto \lambda^{-1}, \quad \sigma \propto \lambda^2 \quad (25)$$

The photon lifetime for a weakly-coupled ring cavity is given by the waveguide loss:  $\tau_{\text{ph}} = 1/\alpha v_g$ . For a coupling efficiency  $\eta$  (related to the intrinsic and loaded  $Q$  by  $\eta = 1 - Q_L/Q_{\text{int}}$ ), we have:

$$\tau_{\text{ph}} = \frac{1 - \eta}{\alpha v_g} \quad (26)$$

#### ACKNOWLEDGMENT

This work is supported (in part) by the German Research Foundation (DFG) within the project: Silicon-on-Insulator based Integrated Optical Frequency Combs. R.H. was supported by the IMPACT Program of the Council of Science, Technology and Innovation (Cabinet Office, Government of Japan) and an appointment to the IC Postdoctoral Research Fellowship Program at MIT, administered by ORISE through U.S. DOE / ODNI.

#### REFERENCES

- [1] V. Brasch, M. Geiselmann, T. Herr, G. Lihachev, M. H. P. Pfeiffer, M. L. Gorodetsky, and T. J. Kippenberg, "Photonic chipbased optical frequency comb using soliton Cherenkov radiation." *Science* vol. 351, no. 6271, pp. 357–360, 2016.
- [2] M. Jankowski, A. Marandi, C. R. Phillips, R. Hamerly, K. A. Ingold, R. L. Byer, and M. M. Fejer, "Temporal simultons in optical parametric oscillators." *Phys. Rev. Lett.*, to be published [arXiv:1707.04611].
- [3] T. Inagaki, K. Inaba, R. Hamerly, K. Inoue, Y. Yamamoto, and H. Takesue, "Large-scale Ising spin network based on degenerate optical parametric oscillators." *Nat. Photonics*, vol. 10, pp. 415–419, 2016.
- [4] K. Kitayama, "Highly stabilized millimeter-wave generation by using fiber-optic frequency-tunable comb generator." *J. Lightw. Technol.*, vol. 15, no. 5, pp. 883–893, 1997.
- [5] H.-J. Song, N. Shimizu, T. Furuta, K. Suizu, H. Ito, T. Nagatsuma, "Broadband-Frequency-Tunable Sub-Terahertz Wave Generation Using an Optical Comb, AWGs, Optical Switches, and a Uni-Traveling Carrier Photodiode for Spectroscopic Applications." *J. Lightw. Technol.*, vol. 26, no. 15, pp. 2521–2530, 2008.
- [6] J. Hansryd, P. Andrekson, M. Westlund, J. Li, and P. Hedekvist, "Fiber-based optical parametric amplifiers and their applications." *IEEE J. Sel. Topics Quantum Electron.*, vol. 8, no. 3, pp. 506–520, 2002.
- [7] S. Zlatanovic, J. S. Park, S. Moro, J. M. Chavez Boggio et al., "Mid-infrared wavelength conversion in silicon waveguides using ultracompact telecom-band-derived pump source." *Nat. Photonics*, 4(8), 561–564, 2010.

- [8] A. C. Turner-Foster, M. A. Foster, J. S. Levy, C. B. Poitras, R. Salem, A. L. Gaeta, and M. Lipson, "Ultrashort free-carrier lifetime in low-loss silicon nanowaveguides." *Opt. Express* vol. 18, no. 4, pp. 3582–3591, 2010.
- [9] A. Gajda, L. Zimmermann, J. Bruns, B. Tillack, and K. Petermann, "Design rules for p-i-n diode carriers sweeping in nano-rib waveguides on SOL." *Opt. Express* vol. 19, no. 10, pp. 9915–9922, 2011.
- [10] L. A. Lugiato and R. Lefever, "Spatial dissipative structures in passive optical systems," *Phys. Rev. Lett.* vol. 58, no. 21, pp. 2209–2211, 1987.
- [11] R. Hamerly, D. Gray, C. Rogers, L. Mirzoyan, M. Namdari and K. Jamshidi, "Optical bistability, self-pulsing and XY optimization in silicon micro-rings with active carrier removal." in *Proc. of SPIE*, San Francisco, CA, 2017, pp. 10098-11
- [12] Q. Lin, O. J. Painter, and G. P. Agrawal, "Nonlinear optical phenomena in silicon waveguides: Modeling and applications." *Opt. Express* vol. 15, no. 25, pp. 16604–16644, 2007.
- [13] S. Malaguti, G. Bellanca, A. de Rossi, S. Combr e, and Stefano Trillo, "Self-pulsing driven by two-photon absorption in semiconductor nanocavities," *Phys. Rev. A* vol. 83, no. 051802(R), 2011.
- [14] R. Hamerly and H. Mabuchi, "Optical Devices Based on Limit Cycles and Amplification in Semiconductor Optical Cavities," *Phys. Rev. Appl.* vol. 4, no. 024016, 2015.
- [15] L. Yin, Q. Lin, and G. P. Agrawal, "Dispersion tailoring and soliton propagation in silicon waveguides," *Opt. Lett.* vol. 31, no. 9, pp. 1295–1297, 2006.
- [16] R. Hamerly, A. Marandi, M. Jankowski, M. M. Fejer, Y. Yamamoto, and H. Mabuchi, "Reduced models and design principles for half-harmonic generation in synchronously pumped optical parametric oscillators," *Phys. Rev. A* vol. 94, no. 063809, 2016.
- [17] R. Hamerly, "Coherent LQG Control, Free-Carrier Oscillations, Optical Ising Machines and Pulsed OPO Dynamics." Ph.D. dissertation, Dept. Appl. Physics, Stanford Univ., CA, 2016.
- [18] X. Liu, R. M. Osgood Jr., Y. A. Vlasov, and W. M. J. Green, "Mid-infrared optical parametric amplifier using silicon nanophotonic waveguides," *Nat. Photonics* vol. 4, pp. 557–560, 2010.
- [19] D. Dimitropoulos, S. Fathpour, and B. Jalali, "Limitations of active carrier removal in silicon Raman amplifiers and lasers," *Appl. Phys. Lett.* vol. 87, no. 261108, 2005.
- [20] C. Jacoboni, C. Canali, G. Ottaviani, and A. A. Quaranta, "A review of some charge transport properties of silicon." *Solid State Electron.* vol. 20, no. 2, pp. 77–89, 1977.



**Ryan Hamerly** was born in San Antonio, Texas in 1988. In 2016 he received a Ph.D. degree in applied physics from Stanford University, California, for work with Prof. Hideo Mabuchi on quantum control, nanophotonics, and nonlinear optics. In 2017 he was at the National Institute of Informatics, Tokyo, Japan, working with Prof. Yoshihisa Yamamoto on quantum annealing and optical computing concepts, and is currently an IC postdoctoral fellow at MIT, Cambridge, Massachusetts, with Prof. Dirk Englund.



**Kambiz Jamshidi** (M'03) received the Ph.D. degree in electrical engineering from Sharif University of Technology (SUT), Tehran, Iran, in 2006. From 2009 to 2013, he worked with the HFT Institute (Deutsche Telekom University of Applied Sciences, Leipzig, Germany) and the Photonics Lab (Technical University of Berlin). He is currently an assistant professor of integrated photonic devices in the Communications Lab at Dresden University of Technology.

**Meysam Namdari, Levon Mirzoyan, Dodd Gray, Christopher Rogers** photographs and biographies not available at time of publication.